JOURNAL OF MATERIALS SCIENCE 17 (1982) 2298–2308

An electrical conductivity and TEM study of the sulphurization by gaseous H_2S of NiO single crystals

C. BOURGEOIS, P. DUFOUR, J. C. MUTIN, A. STEINBRUNN
Laboratoire de Recherche sur la Réactivité des Solides CNRS LA 23, B.P. 138, 21004 Dijon Cedex, France

An electrical conductivity and transmission electron microscopy study of the very early stages of the sulphurization by H_2S of NiO single crystals were carried out at low pressure ($p < 20$ Torr) and at $T < 700$ K. For treatments at $p_{H_2S} < 10^{-4}$ Torr 2 main stages of reaction were found: (a) a topotactical reduction of the oxide producing Ni islands with a diameter of about 20 nm and (b) an epitaxial overgrowth of Ni_3S_2 from the metallic islands. The maximal conversion rate of the NiO sulphurization is very low and depends on the states of the crystal surface. For treatments at $p_{H_2S} \simeq 20$ Torr a non-stoichiometric nickel sulphide was identified.

1. Introduction

The study of the metallic oxide sulphurization by gaseous hydrogen sulphide has been undertaken for a few years in our laboratory. The main interests of this study are the fundamental aspects of these reactions as well as the importance of these interactions for corrosion studies (i.e. the stability of protective oxide layers on metals against sulphur compounds) and for some catalytic reactions in hydrodesulphurization. The present results follows those obtained with oriented monocrystalline faces [1–4]. It deals with the NiO–H_2S interaction at very low conversion rates about which few studies seem to have been performed, as far as we know.

The aim of this work is the study of the germination processes of the sulphurization of NiO by H_2S by electrical conductivity and transmission microscopy.

2. Methods

NiO monocrystals were grown by the Verneuil method from very high purity powder (5N). Their impurity content was less than 100 ppm. The orientation of the crystals was determined by the Laue method and they were then cut with an annular diamond saw into parallelepiped samples (15 mm x 3 mm x 3 mm) or plates (15 mm x 6 mm x 1 mm) with faces parallel to the (1 0 0) crystallographic planes.

Electrical conductivity measurements were made either by the direct current four probe method or by the alternative current two probe method (using a Wahne Kerr Bridge, 1592 Hz). The electrical contacts were made by 4 platinium bowls at the end of the wires connected both to the d.c. power supply and to the high impedance voltmeter. Otherwise the electrical contacts were made by a platinium paste between the crystal and the tightly bound platinium wire which was connected to the resistance bridge. The electrical conductivity was continuously recorded during the various exposures of NiO to the H_2S gas. The samples are maintained in the gas, streamed through a vertical cylindrical quartz tube. The pressure (10^{-5} to 10^{-1} Torr) (1 Torr = 133.3 N m^{-2}) is stabilized by a Knudsen dynamical regime owing to a classical pumping system (10^{-7} Torr) and a leak valve. A cylindrical furnace around the quartz tube is used to heat the samples.

As for the electron microscope investigation, since the *in situ* sulphurization was not possible, the NiO powder previously deposited on Au grids was sulphurated in the conductivity device and

0022–2461/82/082298–11$03.82/0

subsequently observed. The samples were prepared by grinding of single crystals in liquid nitrogen. The NiO crystallites had a quite large defect ratio, which was reduced by annealing the powder for a few hours at 500 K. The defects also mainly disappeared during temperature equilibration of the samples before the sulphurization. This treatment, which was performed for variable times, was stopped by pulling down the cylindrical furnace in order to quench the sample to room temperature.

3. Results

3.1. Isothermal evolution of the electrical conductivity of NiO single crystal exposed to low H_2S pressures. The role of the surface and of the temperature

Measurements of electrical conductivity variations of NiO during its interaction with H_2S streamed at low pressures ($p < 10^{-4}$ Torr) were performed on samples prepared with different surface states in a temperature range which allowed the nucleation and growth of the sulphide ($T < 700$ K).

Fig. 1 shows the relative conductance, G/G_0, evolution against the exposure time for a H_2S pressure of about 1×10^{-4} Torr and for two different surface states. Curve I shows the results obtained with an oxide sample whose surface was prepared by a classical mirror polishing (using diamond paste of successively fine grains, i.e. 10 then 5 then 1 μm). Curve II shows the results obtained with another NiO single crystal whose surface was prepared by nitric acid etching (HNO_3 at 400 K, for 15 min) in order to eliminate the uppermost amorphous NiO layer. These curves show that the relative conductance of NiO does not change at the very beginning. This "induction period" time changes according to the nature of the crystal surface. It is quite long for the chemical etched surface. The relative conductance increases slightly up to a plateau value. For identical exposure times we can notice that:

(a) the relative conductance obtained with the polished sample surface is always higher than the chemical etched surface sample;

(b) the morphology of the surface corresponding to the particular value of the relative conductance is different from one sample to the other.

The scanning electron microscope (SEM) micrographs of Fig. 2 show the growth of Ni_3S_2 crystallites as detected by X-ray diffraction. The relative conductance increase with the H_2S exposure time is due to the superficial growth of this phase. The sulphide layer is much more homogeneous in the case of the polished surface sample than in the case of the chemical etched surface sample. With the former, the curves of Fig. 3 show the expected effect of the temperature increase during the NiO–H_2S interaction. This effect is also observed for the induction period time (H_2S admolecule equilibrium, coalescence kinetics of detectable nuclei) which is 80 min at 540 K, 30 min at 620 K, a few minutes at 650 K, and for the rate of the growth of the superficial sulphide thin film.

3.2. Variation of the electrical conductivity activation enthalpy at the very first stages of the NiO–H_2S interaction

The evolution of the electrical conductivity activation enthalpy of NiO during its sulphuriz-

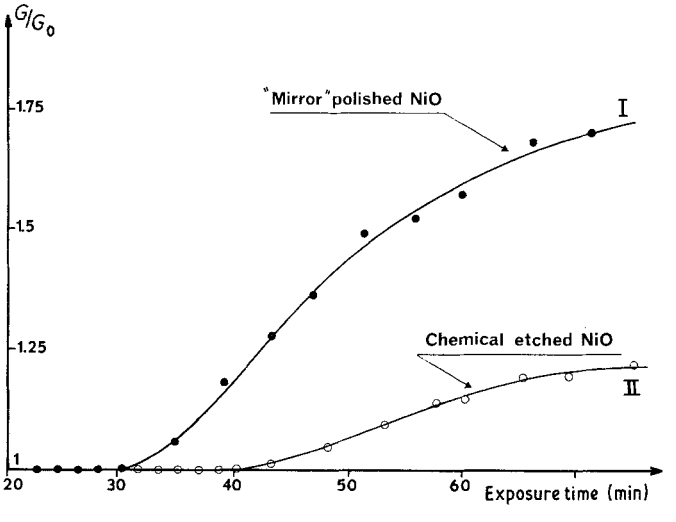

Figure 1 Isothermal variation of the NiO single crystal relative conductance for different surface states against H_2S exposure time at 620 K and $p_{H_2S} = 10^{-4}$ Torr.

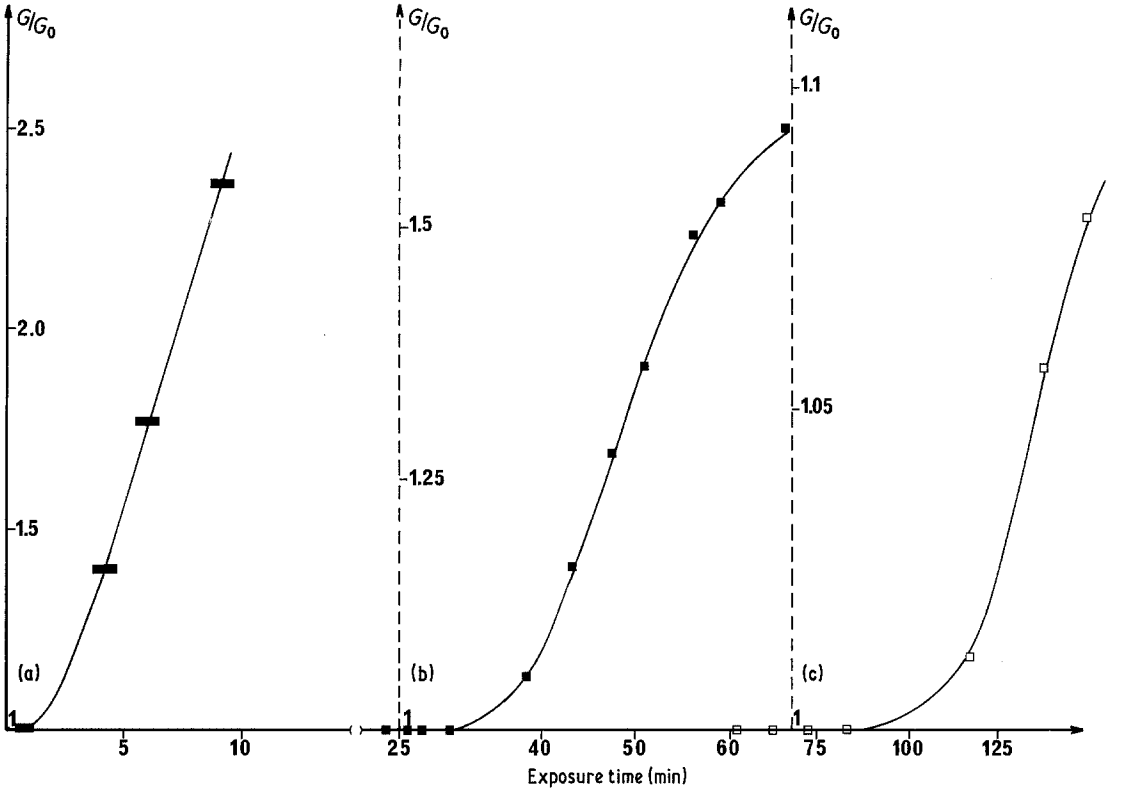

Figure 2 Isothermal variation of the NiO single crystal relative conductance at temperatures of (a) 650 K, (b) 620 K and (c) 540 K against H_2S exposure time ($p_{H_2S} \simeq 10^{-4}$ Torr).

ation by H_2S was studied at different conversion rate of the reaction. Fig. 4 shows the results obtained with 4 successive exposures of increasing time, i.e., 10, 20, 25 and 28 h ($T = 620\,K\, p_{H_2S} = 10^{-4}$ Torr).

After each gas exposure, the single crystal is quenched and then an activation enthalpy measurement is performed by increasing the temperature of the crystal under vacuum (5×10^{-6} Torr). Curve 0, obtained with the clean polished single crystal, shows a characteristic discontinuity at the vicinity of the Néel temperature, T_N. The conductivity activation enthalpy is not constant in the whole temperature range in relation to the antiferromagnetic properties of the oxide. The migration enthalpy of the electronic holes is influenced by the cationic sublattice ordering [5].

Thus substrate characteristic curve is slightly modified by the overgrowth of the sulphide. Curves 1, 2 and 3, recorded for intermediate conversion rates, show that the discontinuity at the vicinity of T_N vanished when the sulphide overlayer is grown at the NiO surface.

For the maximum coverage of the thin film (approximately 300 nm) (Curve 4) the activation enthalpy is very close to that of a metallic conductor (0.08 ± 0.02 eV).

3.3. Transmission electron microscope study of the NiO sulphurization by H_2S

The first sulphurization tests, having shown that the reactivity of the divided oxide is different from that of a large single crystal, we treated NiO samples dispersed on gold grids at higher temperatures, 570 and 620 K. Two sets of tests were selected respectively (570 K, $p_{H_2S} = 10^{-4}$ Torr and 620 K, $p_{H_2S} = 20$ Torr). The microscopic observations and the identification of the different phases were made on samples whose treatment time was increased.

3.3.1. Results concerning the H_2S low pressure (10^{-4} Torr) treatments at 570 K

3.3.1.1. One hour treatment. After one hour the major part of the oxide grains are less transformed. Nevertheless, some of them give a diffraction

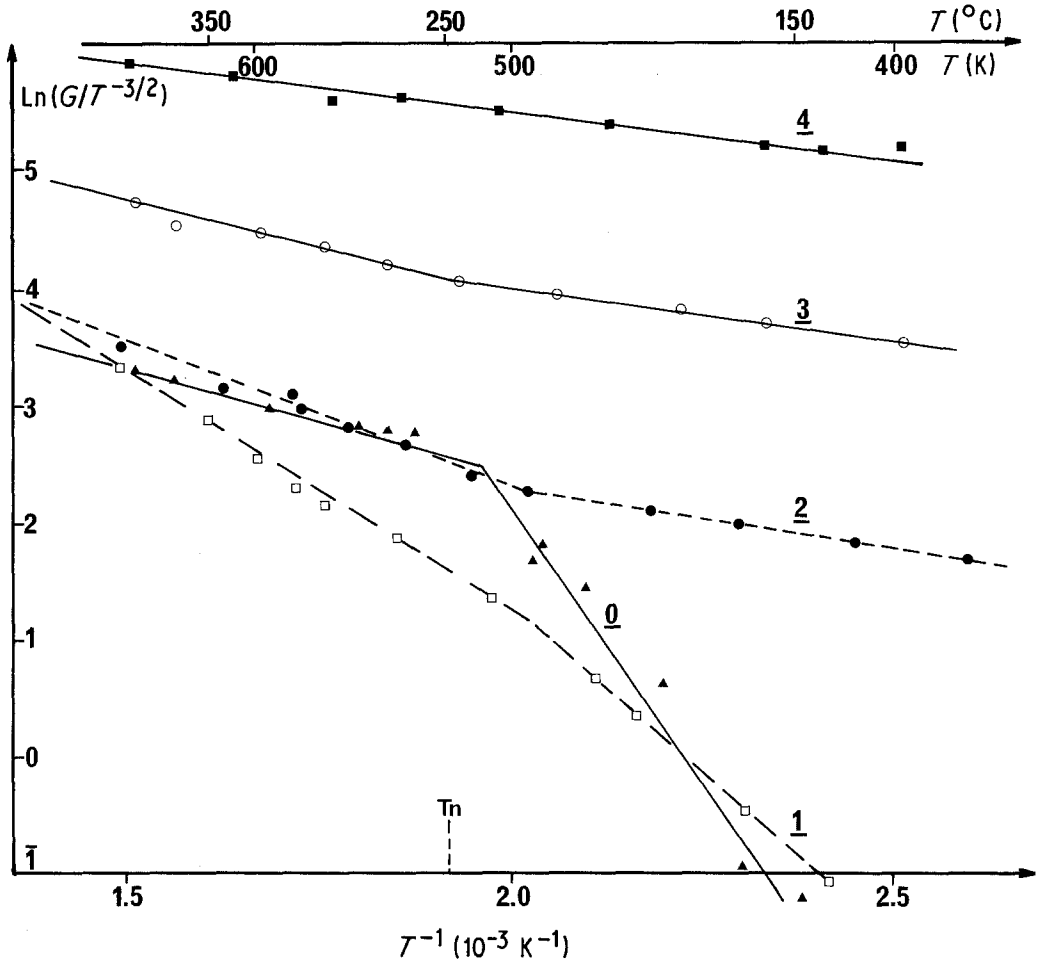

Figure 3 Electrical conductivity activation enthalpy against different very early stages of the sulphurization of a NiO single crystal by H_2S ($T = 620$ K, $p_{H_2S} \simeq 10^{-4}$ Torr). Curve 0 polished (1 0 0) NiO. Curve 1 after a 10 h treatment. Curve 2 after a 20 h treatment. Curve 3 after a 25 h treatment. Curve 4 after a 28 h treatment.

pattern which shows a reduction of the oxide crystallites. Indeed, the diffraction pattern (Fig. 5) shows that the spots of the oxide remain while those of the nickel appear.

The small extra spots arise from double diffraction of the electron beam by the oxide and the metal.

3.3.1.2. 3 hour treatment. After 3 h the diffraction patterns show an important transformation of the nickel oxide. An increase of the reduction (nickel) and the overgrowth of a detectable quantity of sulphide Ni_3S_2 is observed. The orientation of the nickel lattice with respect to that of the nickel oxide is obvious. Fig. 6a comes from a characteristic NiO cleavage plate, (1 0 0). The diffraction pattern shows a three dimensional coincidence of the main axes of the nickel cubic lattice with those of the NiO cubic lattice (Fig. 6b). The orientation relationships are

$$[1\,0\,0]\ \text{Ni} \parallel [1\,0\,0]\ \text{NiO},$$

$$[0\,1\,0]\ \text{Ni} \parallel [0\,1\,0]\ \text{NiO},$$

and consequently

$$[0\,0\,1]\ \text{Ni} \parallel [0\,0\,1]\ \text{NiO}. \qquad (1)$$

These relationships are in agreement with the results of Floquet *et al.* [9].

Moreover, close observation of Fig. 6a shows other weak arced spots close to the NiO and Ni spots. The shape of these reflections prove that the corresponding phase is not as well oriented as the nickel. The main spots which can be detected on the original pattern have been drawn in Fig. 6c. The expected sulphide Ni_3S_2 is identified. Owing

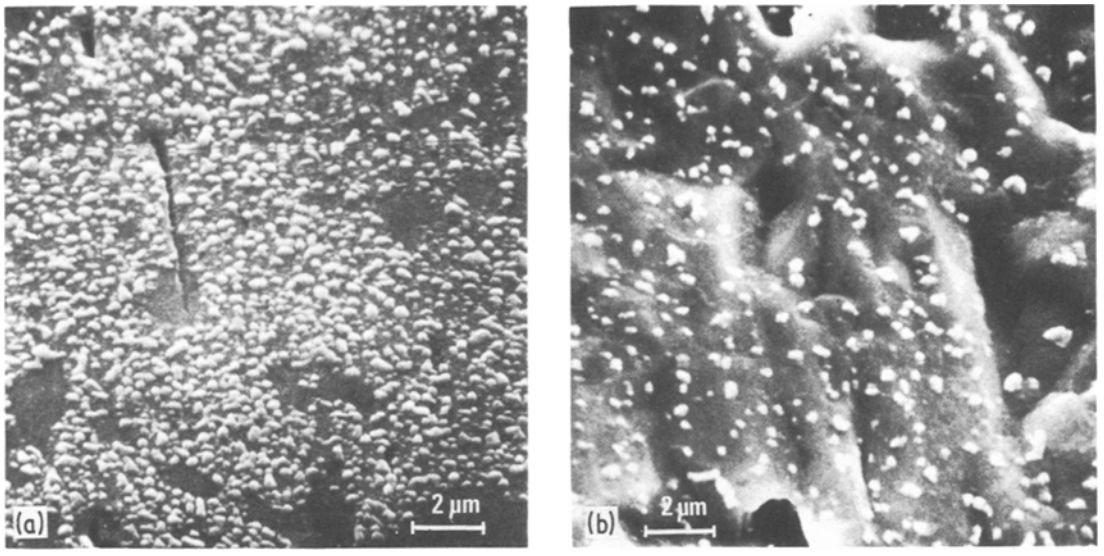

Figure 4 Scanning electron micrographs of the sulphurated NiO surface after a 70 min treatment ($T = 620$ K, $p_{H_2S} \simeq 10^{-4}$ Torr) showing (a) a "polished" NiO surface, (b) a "chemical etched" surface.

to a reflection indexation of the rectangular lattice side view, a lattice coincidence between the NiO lattice (or the Ni which is parallel) and the sulphide can be established.

$$(1\,0\,\bar{1}\,1)\,Ni_3S_2 \parallel (1\,0\,0)\,NiO$$
$$(\bar{1}\,2\,\bar{1}\,0)\,Ni_3S_2 \parallel (0\,1\,0)\,NiO$$
$$[2\,1\,.\bar{2}]\,Ni_3S_2 \parallel [0\,0\,1]\,NiO \qquad (2)$$

Micrographs 6a and 7 show the shape of the partially transformed NiO crystallites. The interpretation of moiré images shows that the nickel, produced by the NiO reduction, grows as individual microcrystallites having all the same orientation in relation to the oxide. The Ni_3S_2 sulphide detected on the diffraction patterns was not observed accurately on the micrographs.

3.3.1.3. 6 hour treatment. The striking observation deduced from the diffraction pattern analysis is that the Ni metallic phase disappears on most preparation grains. The Ni_3S_2 sulphide is only detected and does not show any particular orientation with regard to the substrate. Fig. 8 shows that at this transformation step, the NiO crystallite surface is covered with many crystals without any noticeable shape nor orientation relationships.

3.3.1.4. 24 hour treatment. After 24 h the oxide conversion rate does not seem to be different from the one obtained after the 6 hour treatment. The sulphide Ni_3S_2 and the substrate NiO are the only identified phases. Fig. 9a and b illustrate this observation. From some NiO crystallites, the sulphide shows a preferential orientation. The

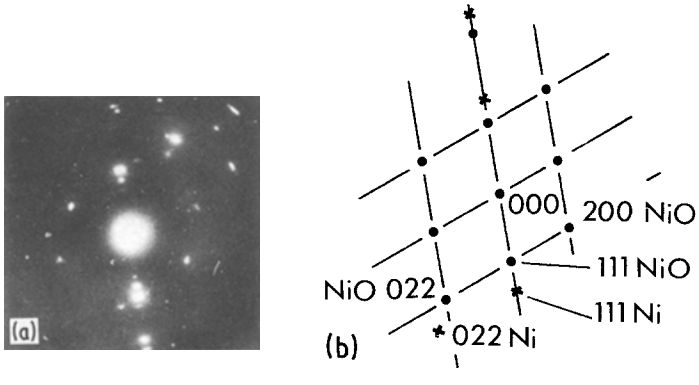

Figure 5 (a) and (b) Diffraction pattern performed on a piece of NiO after a 1 h treatment of sulphurization.

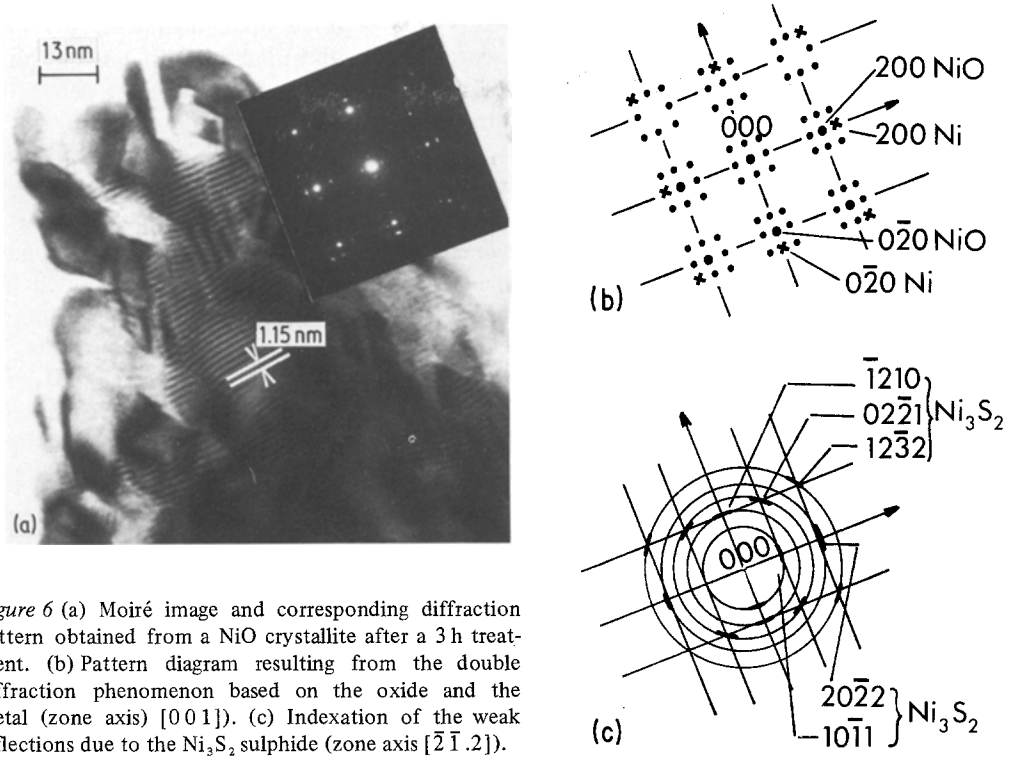

Figure 6 (a) Moiré image and corresponding diffraction pattern obtained from a NiO crystallite after a 3 h treatment. (b) Pattern diagram resulting from the double diffraction phenomenon based on the oxide and the metal (zone axis) [0 0 1]). (c) Indexation of the weak reflections due to the Ni_3S_2 sulphide (zone axis [$\bar{2}$ $\bar{1}$ .2]).

main reflections on the pattern can be indexed from the Ni_3S_2 unit cell. The reciprocal lattice plane is the one obtained with its zone axis [1 0 .$\bar{1}$]. The theoretical angle between the (1 0 $\bar{1}$ 1) and (1 $\bar{3}$ 2 1) planes is 90°8′. The spots on one axis are the harmonics $h\,o\,\bar{h}\,l$. The fact that the $h\,o\,o$ harmonics of the oxide are very close to those ones suggests the following orientation relationship

$$(1\,0\,\bar{1}\,1)_{Ni_3S_2} \parallel (1\,0\,0)_{NiO}$$

$$(1\,\bar{3}\,2\,1)_{Ni_3S_2} \parallel (0\,1\,0)_{NiO}$$

and consequently

$$[1\,0\,.\bar{1}]_{Ni_3S_2} \parallel [0\,0\,1]_{NiO} \qquad (3)$$

These relationships are different from those established by Fig. 10, but the coincidence between the (1 0 $\bar{1}$ 1) sulphide plane and the (1 0 0) oxide plane is still valid.

3.3.2. Results concerning the high pressure (20 Torr) treatments at 570 K

As the last two experiments made at low H_2S

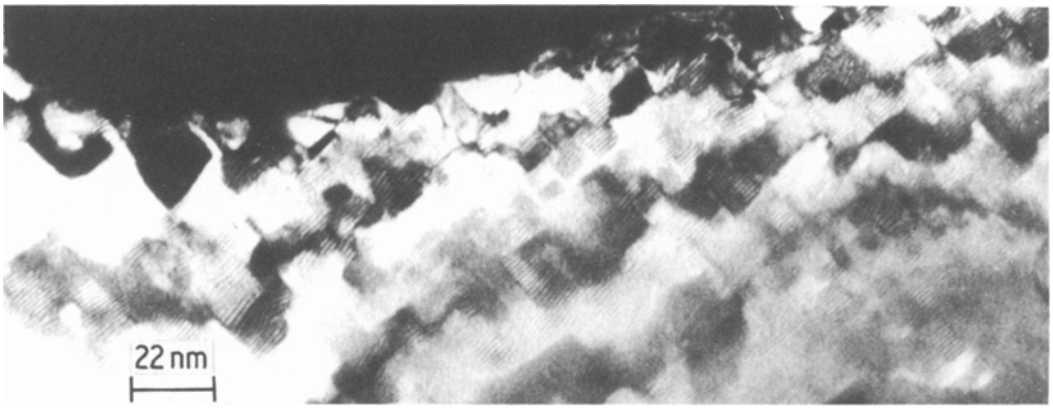

Figure 7 Dark-field picture of a NiO crystallite after a 3 h treatment. The nickel microcrystallites have all the same shape, the same dimensions and a unique orientation.

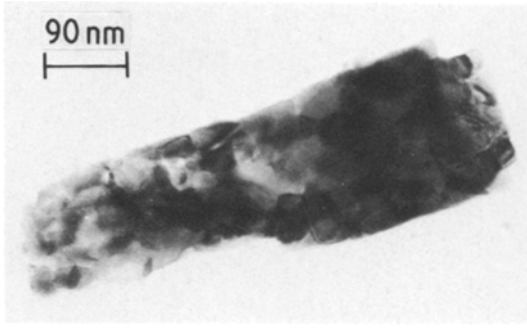

Figure 8 NiO crystallites after a 6 h treatment.

pressure showed a stop in the sulphurization reaction, other tests were performed by changing either the temperature or the gaseous pressure. A modification in the crystallographical and morphological characteristics of the sulphurization products was observed only at 620 K under 20 Torr H_2S.

The main experimental facts which could be observed are:

(a) after a three hour treatment, the oxide seems to be entirely modified into only one phase. The NiO and Ni phases were never detected in micro-diffraction;

(b) the morphological modifications appearing here and there in the NiO grains are visible in Figs 11 to 14. Two kinds of modifications are generally observed. With the thickest oxide grains the reaction product grows as misoriented individual crystallites. Their orientation prevents the transmission of the electron beam. However, the crystallites visible at the edge of the NiO grains have varied but rather well defined shapes (Figs 11 and 12). With the smaller grains, the transformation differ as there is no external growth shape (Figs 13 and 14).

(c) from the morphological observations we could assume the formation of several phases. But, in fact, the micro-diffraction analysis systematically performed indicates the opposite. The quasi totality of the diffraction patterns can be inter-

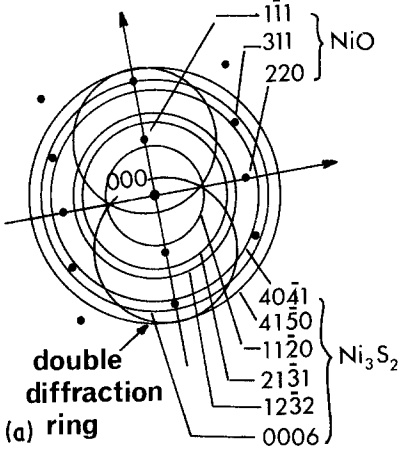

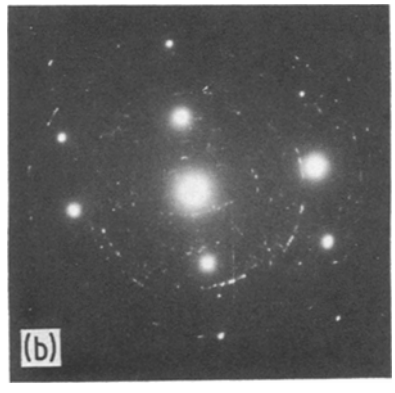

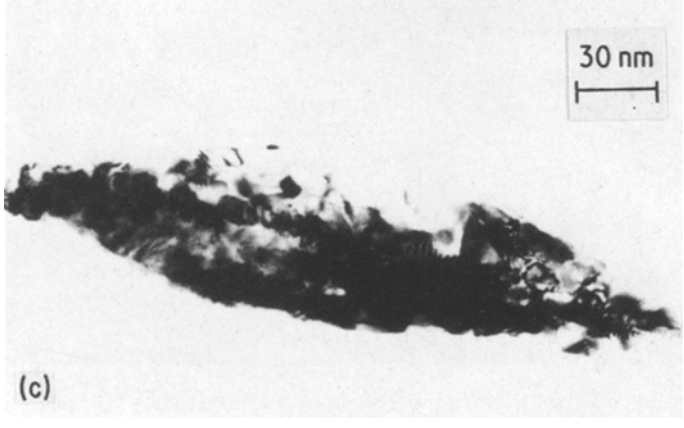

Figure 9 (a) and (b) Diffraction pattern obtained from NiO crystallites (c) after a 24 h treatment. The Ni_3S_2 sulphide covers the oxide.

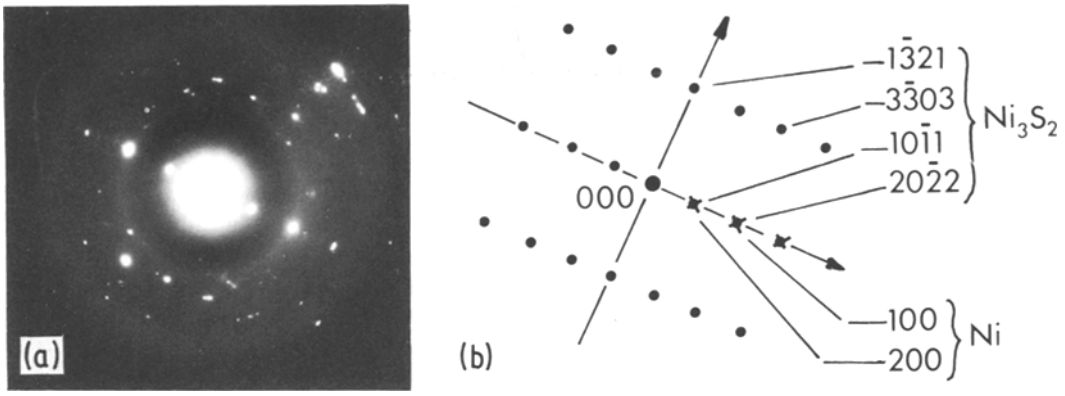

Figure 10 (a) and (b) Diffraction patterns of NiO treated for 24 h at 570 K ($p_{H_2S} = 10^{-4}$ Torr). One can precisely determine, in some cases, the orientation relationships between sulphide and oxide (zone axis of Ni_3S_2 [1 0 .1]).

preted when we consider a cubic cell with a parameter $a = 0.834$ nm. The sulphide formed, called "X", could not be identified with one of the tabulated nickel sulphides. Its structure is close to that of Ni_3S_4 as this was corroborated by the X-ray diffraction diagram recorded from oxide powder treated in the same conditions;

(d) several diffraction patterns display superstructure reflections.

4. Discussion

One may wonder about the use of an analysis made both with monocrystalline faces and with oxide powder crystallites. Two reasons led to this choice. On one hand, LEED* and RHEED† observations had to be checked and completed by an adequate method sensitive to the surface state modifications. These ones give no precise information about the superficial reaction kinetics. On

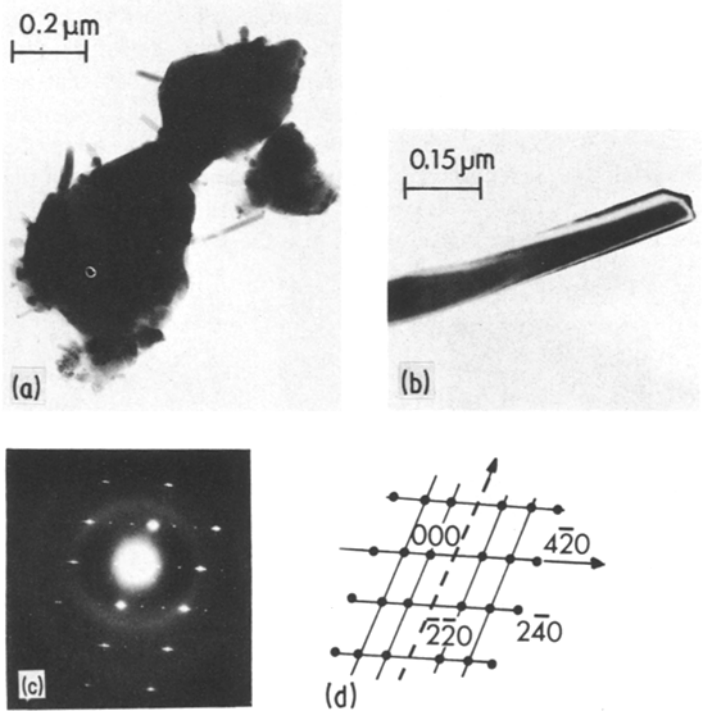

Figure 11 (a) and (b) NiO crystallites visible at the edge of the thick oxide grains after a 6 h sulphurization at $T = 640$ K and $p_{H_2S} \simeq 20$ Torr, and (c) and (d) the diffraction pattern (zone axis [0 0 1] obtained from the needle shown in (b).

*LEED – low energy electron diffraction.
†RHEED – reflection high energy diffraction.

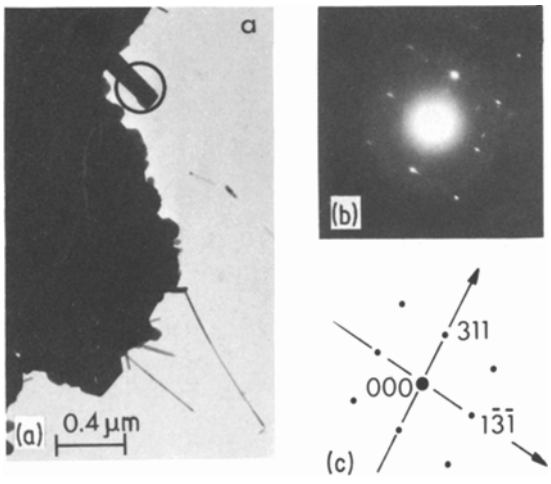

Figure 12 (a) NiO crystallites under the same conditions as Fig. 11. The diffraction pattern, (b) and (c), corresponds to the sulphide crystallite ringed in (a) (zone axis [1 $\bar{2}$ 5]).

the other hand, it is interesting to compare the characteristics (i.e. nature of the products, the steps of the reaction, morphology and crystallography) of the reaction of the oxide as a powder or as a monocrystalline phase, this kind of observation being important for the study of industrial catalysts.

4.1. Conductivity measurements and overgrowth kinetics of the thin films

The measurements of the NiO electrical conductivity during the H_2S interaction enable us to follow continuously the overgrowth of the sulphide thin film. The aspect of the curves on Fig. 1 can be interpreted by the fact that the phase conductivity which occurs during the NiO–H_2S interaction is higher than that of the substrate ($10^{+4}\ \Omega\ cm^{-1}$ for Ni and Ni_3S_2 as opposed to $10^{-6}\ \Omega\ cm^{-1}$ for NiO). As soon as the metal or sulphide islands nucleate, the relative conductance, G/G_0, increases. When the island coverage is high enough to form a quasi-continuous thin film G/G_0 tends to a limiting value. This effect is particularly outlined on the curves of Fig. 3. The curve shows for $T < T_N$ a decrease of the activation enthalpy which can be explained by the electrical conductivity theory of discontinuous thin films [6, 7]. The changes of the crystal forms could be the cause of the total decrease of the conductivity whereas their coalescence could explain the diminishing activation enthalpy of the conductivity.

The conductivity experimental results bring two comments:

(a) the thickness of the sulphide film which is formed when the plateau value of G/G_0 is reached, corresponds to a conversion rate of a few hundredth percent. This proves the sensitivity of the technique as well as its complementarity to the surfac analysis technique (LEED, RHEED, AUGER);

(b) however, the electrical conductivity measurements do not reveal the nature of the phases formed. The reduction step observed by the diffraction techniques was not detected. This deficiency can be explained by the fact that the metal and sulphide conductivities have very similar values, which prevents us from discerning the reduction step from the sulphurization step on the $G/G_0 = f(t)$ curves. The lifetime of the metallic phase is likely to be very short.

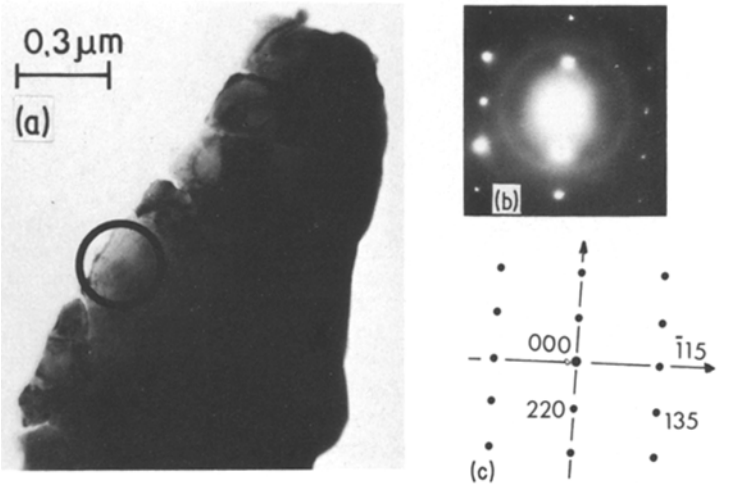

Figure 13 The smallest NiO crystallites in the same NiO sample as Fig. 11 showing (a) no change in initial morphology after sulphurization. The [5 5 2] zone axis diffraction pattern, (b) and (c), show however that the sulphide obtained is identical with that in Figs 11 and 12.

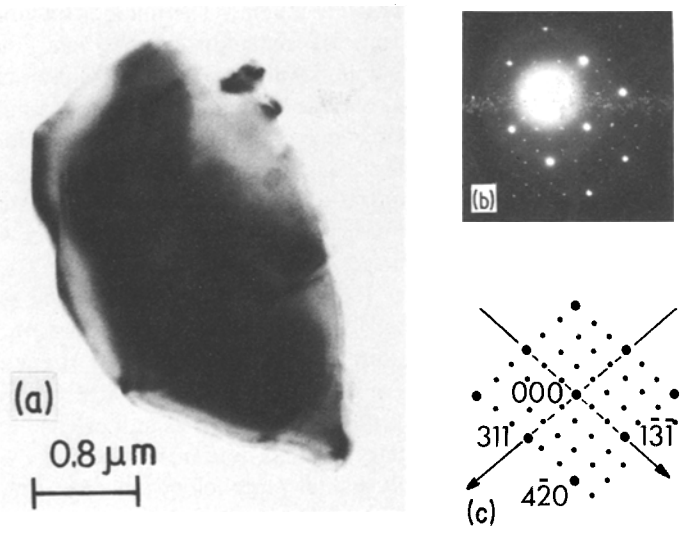

Figure 14 (a) A small NiO crystallite in the same NiO sample as Fig. 11 and (b) and (c) the [1 $\bar{2}$ 5] zone axis diffraction pattern, showing again that the sulphide obtained is identical with that in Figs 11 and 12.

4.2. Comparison between the reactivity of the monocrystalline faces and the microcrystallites of the NiO powder

The results mentioned above and concerning the treatment of the NiO powder under 10^{-4} Torr H_2S agree with the LEED, RHEED and Auger observations of monocrystalline faces [2]. They definitely confirm that:

(a) the initial step of the NiO–H_2S interaction consists in a reduction of the oxide and the formation of nickel individual microcrystallites. The three dimensional orientation of the lattices of the two phases is also the one obtained from the LEED and RHEED patterns. The optical micrographs complete these observations and show the flat shaped Ni crystallites at the NiO surface. The regularity of both orientation and morphology of these crystallites allows us to assume that the reduction is topotactic, i.e., it does not involve the diffusion of the Ni atoms;

(b) the formation of Ni_3S_2 occurs as soon as the metal appears. This sulphide is indeed detected by microdiffraction at the very beginning of the NiO–H_2S interaction. When the treatment is continued the evolution then shows that Ni_3S_2 grows from the metal and not from the oxide. On the other hand, the electronic microdiffraction patterns do not enable us, for two reasons, to assert that there is a systematic orientation between the sulphide and the oxide lattice: firstly, the patterns giving orientation relationship between the two phases are not numerous and Debye–Sherrer rings patterns were more often observed and, secondly, the orientation relationships which could be established are not similar from one sample to another. Moreover the most likely coincidence (cf. relationships 2 and 3) applies to the planes NiO (1 0 0) and Ni_3S_2 (1 0 $\bar{1}$ 1). It is different from what was observed by LEED ($(0\,1\,0)_{NiO} \parallel (1\,1\,\bar{2}\,0)_{Ni_3S_2}$) but this however appears in the relationships obtained from patterns realized on NiO grains weakly sulphurated on which the sulphide and the metal coexist.

4.3. Identification of sulphide "X" produced during the sulphurization under 20 Torr H_2S

The results of the microdiffraction analysis clearly show that the phase produced in such conditions is not the expected one i.e. the rhombohedral sulphide NiS (millerite). However they do show the growth of a cubic phase similar to Ni_3S_4 thanks to the symmetry of its unit cell. The stoichiometry of this phase could not be determined by thermogravimetric analysis, but a simple crystallographic argument enables us to locate it between Ni_3S_4 and NiS. Table I gives the multiple cell parameters (f c c or hexagonal) and those of the unit cell (rhombohedral) of Ni_3S_4, "X" and NiS.

We notice that the "X" phase can be described as a sulphide which looks like a non-stoichiometric NiS thanks to the parameters of its unit cell (the Ni vacancies rate can reach 6% according to Laffite [8]) and by its lattice symmetry, which is not far from Ni_3S_4.

The hypothesis of a non-stoichiometric phase is confirmed by the presence of extra very sharp reflections in a great number of patterns. This

TABLE I Cell parameters of various Ni–S phases

Phase	Crystal system	Multiple cell parameters (nm)	Unit cell parameters*
Ni_3S_4	fcc (Fd3m)	$a = 0.948$	$a = 0.670$ $\alpha = 60$
"X"	fcc (Fd3m)	$a = 0.834$	$a = 0.590$ $\alpha = 60$
NiS	hexagonal (R3m)	$a = 0.962$ $c = 0.315$	$a = 0.565$ $\alpha = 63.42$

*a in nm, α in °.

diffraction phenomenon reveals the presence of a 3-fold superstructure compatible with an ordered distribution of the Ni vacancies.

5. Conclusion

As a conclusion of this study of the NiO–H_2S interaction at very low conversion rate we have pointed out that:

(a) electrical conductivity measurements are able to follow continuously the superficial electrical properties of the solid during the solid–gas interaction;

(b) an "induction" period between the time of exposure and the observation of an increase of the relative conductance was detected. It is due mainly to the time needed to build up an equilibrium concentration of H_2S admolecules on the NiO surface and to the time required by the underneath solid to equilibrate its defects concentration;

(c) the state of the crystal surface influences the "induction" period and consequently the solid reactivity;

(d) electron microscopy observations confirm the sulphurization stages already observed by LEED and RHEED studies. The microdiffraction patterns detect the reduction of NiO and the subsequent sulphurization of the Ni islands. The micrographs obtained specify the topotactic character of the reduction (shape and dimension of the metallic islands) and put in evidence a stop of the sulphurization for very low conversion rate: the whole nuclei being located at the vicinity of the crystal surface.

For higher H_2S pressure treatments the transformation characteristics are different because of:

(a) the nature of the sulphide phase formed, "X", (which was determined as non-stoichiometric NiS thanks to the parameters of its unit cell and its lattice symmetry which is not far from Ni_3S_4);

(b) the crystallite morphology of this non-stoichiometric sulphide.

The nucleation stage is definitively determining for the nature of the sulphide phase formed.

References

1. A. STEINBRUNN, P. DUMAS and J. C. COLSON, *Surface Sci.* **74** (1978) 201.
2. A. STEINBRUNN, Sc.D. Thesis, Dijon (1979).
3. A. STEINBRUNN and P. DUMAS, *Le Vide, Les Couches Minces* **201** (1980) 1384.
4. P. DUMAS, A. STEINBRUNN and J. C. COLSON, *Thin Solid Films* **79** (1981) 267.
5. A. STEINBRUNN and C. BOURGEOIS, *J. Phys. Chem. Solids* **43** (1982).
6. J. E. MORRIS and T. J. COUTTS, *Thin Solid Films* **47** (1977) 1.
7. T. J. COUTTS, *ibid.* **38** (1976) 313.
8. M. LAFFITE, Sc.D. Thesis, Paris (1958).
9. N. FLOQUET, P. DUFOUR and L. C. DUFOUR, *J. Microscopie Spectroscopie Electronique* **6** (1981) 473.

Received 23 November
and accepted 15 December 1981